scientific reports

Check for updates

OPEN

Structural and biochemical analyses of the flagellar expression regulator DegU from *Listeria monocytogenes*

Han Byeol Oh, Su-jin Lee & Sung-il Yoon✉

Listeria monocytogenes **is a pathogenic bacterium that produces flagella, the locomotory organelles, in a temperature-dependent manner. At 37 °C inside humans, *L. monocytogenes* employs MogR to repress the expression of flagellar proteins, thereby preventing the production of flagella. However, in the low-temperature environment outside of the host, the antirepressor GmaR inactivates MogR, allowing flagellar formation. Additionally, DegU is necessary for flagellar expression at low temperatures. DegU transcriptionally activates the expression of GmaR and flagellar proteins by binding the operator DNA in the *fliN-gmaR* promoter as a response regulator of a two-component regulatory system. To determine the DegU-mediated regulation mechanism, we performed structural and biochemical analyses on the recognition of operator DNA by DegU. The DegU-DNA interaction is primarily mediated by a C-terminal DNA-binding domain (DBD) and can be fortified by an N-terminal receiver domain (RD). The DegU DBD adopts a tetrahelical helix-turn-helix structure and assembles into a dimer. The DegU DBD dimer recognizes the operator DNA using a positive patch. Unexpectedly, unlike typical response regulators, DegU interacts with operator DNA in both unphosphorylated and phosphorylated states with similar binding affinities. Therefore, we conclude that DegU is a noncanonical response regulator that is constitutively active irrespective of phosphorylation.**

Listeria monocytogenes is a gram-positive, nonspore-forming bacterium that is ubiquitously found in water, soil, plant vegetation, and animal feces and grows in a wide range of temperatures and even in low-pH and high-salt environments[1–3]. This robust bacterium contaminates most foods, including dairy products and meats, and can cause food-borne gastroenteritis or more severe diseases, such as sepsis, meningitis, and encephalitis, in humans[4–6]. *L. monocytogenes* is motile both in the environment and hosts using different locomotion modes[7,8]. At temperatures below 30 °C, *L. monocytogenes* generates flagella and moves by rotating them. However, at 37 °C in human hosts, *L. monocytogenes* stops flagellar expression and obtains locomotive force by polymerizing host actin proteins.

In *L. monocytogenes*, flagellar expression is controlled via three regulatory proteins, MogR, GmaR, and DegU[9–14]. MogR functions as a negative transcriptional regulator of all flagellar genes, and its repression activity is especially important for inhibiting flagellar production at 37 °C[12,13,15]. At or below 30 °C, GmaR binds and inactivates MogR, relieving the MogR-mediated repression of flagellar transcription[10,12]. DegU is also required to derepress flagellar transcription because DegU transcriptionally promotes GmaR expression by recognizing the operator site in the *fliN-gmaR* promoter[12,14]. Moreover, DegU directly enhances the transcription of several flagellar genes. Thus, DegU is considered a positive regulator of motility.

A two-component regulatory system (TCS) is generally used by bacteria to detect and respond to changes in the environment and cell[16,17]. The TCS typically consists of a histidine kinase and a response regulator. The histidine kinase functions as a sensor and undergoes autophosphorylation at a conserved histidine residue in response to a signal. Subsequently, the histidine kinase phosphorylates the response regulator by transferring its phosphate group to a conserved aspartate residue in the response regulator. Upon phosphorylation, the response regulator generally changes its binding affinity for the cognate operator DNA and controls genetic transcription. Interestingly, *L. monocytogenes* DegU (lmDegU) is an orphan response regulator. *L. monocytogenes* lacks the

Division of Biomedical Convergence, College of Biomedical Science, Kangwon National University, 1 Kangwondaehak-gil, Biomedical Science Building A-204, Chuncheon 24341, Republic of Korea. ✉email: sungil@kangwon.ac.kr

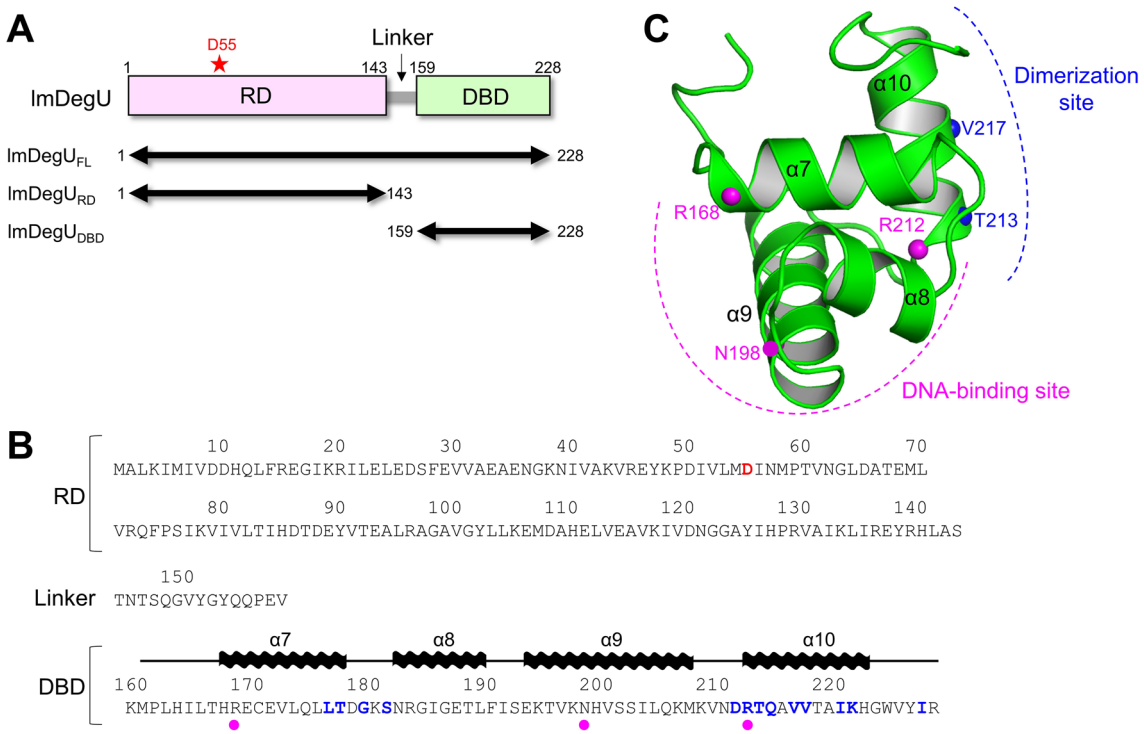

Figure 1. Domain organization of lmDegU and overall structure of lmDegU$_{DBD}$. (**A**) Domain organization and expression constructs of lmDegU. The phosphorylation site of lmDegU (D55 residue) is indicated by a red star. (**B**) Amino acid sequence of lmDegU. The α-helices of the lmDegU$_{DBD}$ structure are represented by waves above the lmDegU sequence, and the remaining region defined in the lmDegU$_{DBD}$ structure is shown as lines. The phosphorylation site (D55 residue) and dimerization interface residues of lmDegU are colored red and blue, respectively. The three lmDegU residues (R168, N198, and R212), which were mutated to confirm their critical roles in dsDNA binding, are indicated by magenta circles. (**C**) Overall structure of a lmDegU$_{DBD}$ monomer (chain A). The lmDegU$_{DBD}$ structure is shown as green ribbons. The T213 and V217 residues, which were mutated to confirm the dimerization interface of lmDegU$_{DBD}$, are shown as blue spheres. The R168, N198, and R212 residues of lmDegU, which were mutated to confirm their critical roles in dsDNA binding, are indicated by magenta spheres.

gene for the histidine kinase that phosphorylates DegU although the DegU-activating histidine kinase (DegS) has been identified in other gram-positive bacteria, such as *Bacillus subtilis*[14,18–20].

Most response regulators are inactive in an unphosphorylated state and become activated upon phosphorylation. However, lmDegU upregulates the expression of motility genes even in an unphosphorylated state, given that the unphosphorylated lmDegU mutant still functions as a positive regulator of motility genes[9,12,21]. It is unclear how lmDegU can activate transcription even in an unphosphorylated state. Based on our structural and biochemical analyses of lmDegU using its diverse constructs and mutants, we provide the molecular mechanism in which lmDegU recognizes its operator DNA in the *fliN-gmaR* promoter and coordinates its DNA-binding activity in a domain-dependent manner. Furthermore, we demonstrate that lmDegU is a unique response regulator that exhibits significant operator DNA-binding affinity in an unphosphorylated state and does not modulate the affinity for the operator DNA in response to phosphorylation.

Results

Overall structure of the DNA-binding domain of lmDegU. lmDegU contains an N-terminal receiver domain (RD; residues 1–143) and a C-terminal DNA-binding domain (DBD; residues 159–228), which are connected by a 15-residue linker (residues 144–158) (Fig. 1A,B and Supplementary Fig. S1). For a structural study of lmDegU to investigate operator DNA recognition by lmDegU, we expressed and purified the full-length, RD, and DBD proteins of lmDegU (lmDegU$_{FL}$, lmDegU$_{RD}$, and lmDegU$_{DBD}$, respectively). The lmDegU$_{DBD}$ protein yielded crystals that could be diffracted. The crystal structure of lmDegU$_{DBD}$ was determined by molecular replacement and was refined to an R_{free} value of 25.3% for the X-ray diffraction data with a resolution of up to 2.39 Å (Fig. 1C, Supplementary Fig. S2, and Supplementary Table S1). The asymmetric unit of the lmDegU$_{DBD}$ crystal contains two lmDegU$_{DBD}$ chains (chains A and B), which have essentially identical structures with a root-mean-square deviation value of 0.50 Å (Supplementary Fig. S3).

lmDegU$_{DBD}$ adopts a one-domain structure with a tetrahelical helix-turn-helix (HTH) motif as observed for a LuxR-type DNA-binding HTH domain that belongs to the GerE (PF00196) family in the Pfam database (Fig. 1C)[22]. The lmDegU$_{DBD}$ structure consists of four α-helices (α7, α8, α9, and α10), and the two adjacent helices are linked by a 3–4 residue loop. The four α-helices of lmDegU$_{DBD}$ are tethered together through interhelix

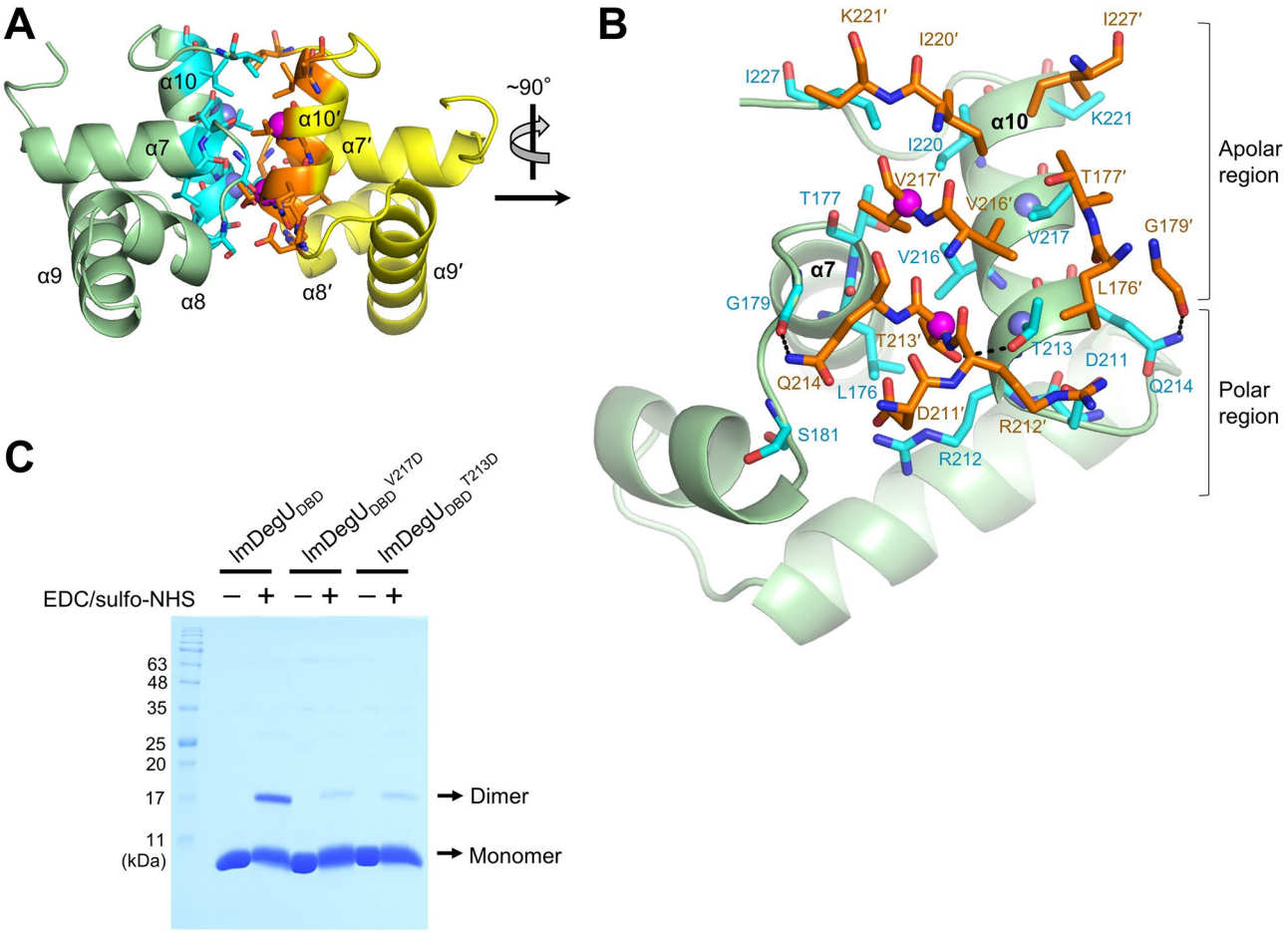

Figure 2. lmDegU$_{DBD}$ dimerization. (**A**) Dimeric structure of lmDegU$_{DBD}$. The dimerization interface residues of lmDegU$_{DBD}$ are shown as cyan and orange sticks in the lmDegU$_{DBD}$ dimer structure (green and yellow ribbons). The T213 and V217 residues, which were mutated to confirm the dimerization interface of lmDegU$_{DBD}$, are highlighted by light blue or magenta spheres. (**B**) lmDegU$_{DBD}$ residues in the dimerization interface. The dimerization interface residues from lmDegU$_{DBD}$ chains A and B are shown as cyan and orange sticks, respectively. lmDegU$_{DBD}$ chain A is depicted as green ribbons. Intermolecular hydrogen bonds are represented by dashed lines. The T213 and V217 residues, which were mutated to confirm the dimerization interface of lmDegU$_{DBD}$, are highlighted by light blue or magenta spheres. (**C**) lmDegU$_{DBD}$ dimerization and its disruption by the mutation of dimerization interface residues (T213D and V217D). lmDegU$_{DBD}$ or its mutant was crosslinked using EDC and sulfo-NHS and analyzed by SDS-PAGE. Protein bands were identified by Coomassie brilliant blue staining. The gel image is representative of three independent experiments that yielded similar results. The full-length gel is shown in Supplementary Fig. S10. The V217D and T213D mutations do not seem to significantly modulate the folding of the lmDegU$_{DBD}$ protein, as lmDegU$_{DBD}^{V217D}$ and lmDegU$_{DBD}^{T213D}$ displayed CD spectra similar to that of lmDegU$_{DBD}$ (Supplementary Fig. S6). Moreover, lmDegU$_{DBD}^{V217D}$ and lmDegU$_{DBD}^{T213D}$ were eluted as single peaks in gel-filtration chromatography in elution volumes similar to that of lmDegU$_{DBD}$ (Supplementary Fig. S5).

hydrophobic interactions and assemble into a short rod-shaped structure. In the lmDegU$_{DBD}$ structure, the α9 helix is the most elongated helix with 15 residues and forms a base frame that supports the other three shorter α-helices. The α9 helix is defined as a recognition helix, which has been shown to be required for dsDNA binding in GerE family members[23].

lmDegU$_{DBD}$ dimerization. Two polypeptide chains in the asymmetric unit of the lmDegU$_{DBD}$ crystal form a dimer (Fig. 2A). The dimerization interface of lmDegU$_{DBD}$ (buried surface area, ~ 500 Å^2) is mainly located at the α10 helix with additional contributions from the C-terminal region of the α7 helix and the α7-α8 and α9-α10 loops (Figs. 1B and 2A). The α10 helix is parallelly aligned with its equivalent helix from the dimerization partner (α10′; the primer denotes the second lmDegU$_{DBD}$ chain in the dimer structure) and is responsible for ~ 64% of the dimerization interface. The dimerization interface of lmDegU$_{DBD}$ is constituted by apolar and polar residues, which are primarily separated into the upper and lower regions of the dimerization interface, respectively (Fig. 2B). Noticeably, the G179 residue in the dimerization interface is most conserved in GerE family sequences and can be defined as a canonical residue of the GerE family (Supplementary Fig. S4). The G179 residue at the α7-α8 loop also functions as a structural residue that is required for the α7-α8 loop to form a sharp turn.

The dimer formation of $lmDegU_{DBD}$ was verified in solution by a chemical crosslinking experiment (Fig. 2C). SDS-PAGE analysis of the crosslinked and non-crosslinked $lmDegU_{DBD}$ proteins indicated that the molecular size of $lmDegU_{DBD}$ shifted to that of a dimer in the presence of crosslinking reagents. However, the dimerization affinity of $lmDegU_{DBD}$ seems to be low, given that the dimeric form of $lmDegU_{DBD}$ was not detected in gel-filtration chromatography, which cannot identify low-affinity interactions (Supplementary Fig. S5). Consistently, the $lmDegU_{DBD}$ dimer has a relatively small buried surface area of ~ 500 $Å^2$.

To confirm the dimerization interface found in the $lmDegU_{DBD}$ crystal, the T213 and V217 residues located in the center of the $lmDegU_{DBD}$ dimerization interface were individually mutated to a larger negatively charged residue, aspartate (Fig. 2A,B). The mutation was expected to disrupt the apolar interaction in the dimerization interface of $lmDegU_{DBD}$. Indeed, in the crosslinking experiment, the $lmDegU_{DBD}^{V217D}$ and $lmDegU_{DBD}^{T213D}$ mutants exhibited substantially lower dimerization efficiencies than $lmDegU_{DBD}$ (Fig. 2C and Supplementary Fig. S6). However, when the $lmDegU_{DBD}$ residues that are located at the periphery of the dimerization interface (R212) or outside the dimerization interface (R168 and N198) were mutated, the dimerization efficiency of $lmDegU_{DBD}$ did not change (Fig. 1B and Supplementary Fig. S7). These results demonstrate that the central dimerization interface of $lmDegU_{DBD}$, involving the T213 and V217 residues, plays a key role in $lmDegU_{DBD}$ dimerization.

DNA recognition by lmDegU using the DBD. lmDegU was shown to interact with the operator site in the *fliN-gmaR* promoter[12]. To examine whether lmDegU employs its DBD to interact with the operator dsDNA, a fluorescence polarization (FP) assay was performed using the fluorescein-labeled operator dsDNA that contains a palindromic sequence from the *fliN-gmaR* promoter (Fig. 3A). The $lmDegU_{DBD}$ protein interacted with dsDNA but with a relatively low binding affinity (dissociation constant K_d, 6.7 ± 2.3 μM). Given that $lmDegU_{DBD}$ binds the palindromic DNA sequence, it is highly likely that $lmDegU_{DBD}$ recognizes dsDNA as a dimeric form. To examine whether $lmDegU_{DBD}$ employs its dimeric structure for the dsDNA interaction, the $lmDegU_{DBD}^{T213D}$ and $lmDegU_{DBD}^{V217D}$ mutants that are deficient in dimerization were subjected to an FP assay (Fig. 3B). Both the $lmDegU_{DBD}^{T213D}$ and $lmDegU_{DBD}^{V217D}$ mutants displayed lower dsDNA-binding activity than the dimerization-competent $lmDegU_{DBD}$ protein, indicating that the dimeric assembly and organization observed in the crystal structure of $lmDegU_{DBD}$ are utilized to achieve the optimal interaction of lmDegU with dsDNA.

To be consistent with the dsDNA-binding ability of $lmDegU_{DBD}$, the $lmDegU_{DBD}$ dimer structure displays a continuous positive patch that is electrostatically complementary to the negatively charged dsDNA (Fig. 3C). To address the DNA-binding mode of lmDegU, we overlaid the $lmDegU_{DBD}$ dimer structure on the DBD of the lmDegU homolog DosR ($DosR_{DBD}$) in complex with dsDNA and generated a $lmDegU_{DBD}$-dsDNA model by combining the $lmDegU_{DBD}$ structure with the dsDNA structure from the $DosR_{DBD}$-dsDNA complex (Fig. 3D)[24]. In the 2:1 $lmDegU_{DBD}$-dsDNA model, dsDNA resides on the positive patch of the $lmDegU_{DBD}$ dimer structure (Fig. 4A). In particular, the α9 recognition helix is inserted into the major groove of dsDNA and appears to play a critical role in dsDNA recognition (Fig. 3D). The positively charged K194 and K197 residues from the α9 helix are located in the positive patch and interact with the DNA bases in the major groove of dsDNA in the complex model (Fig. 4A,B). The neutral hydrophilic residue N198 at the periphery of the positive patch from the α9 helix also seems to function as a DNA base binder. In addition to α9-helix residues, several lmDegU residues from the α7 and α10 helices and their neighboring loops contribute to the interaction of lmDegU with the backbone of dsDNA. In the complex model, the positively charged R168 and R212 residues from the α7 and α10 helices, respectively, make contacts with the backbone of dsDNA. These five lmDegU residues (R168, K194, K197, N198, and R212) are highly conserved in lmDegU orthologs (Supplementary Fig. S1). Notably, among the putative dsDNA-binding residues, the lmDegU R168 residue is conserved as a positively charged residue (arginine or lysine) even across GerE family sequences, suggesting that the R168 residue is indispensable for sequence-independent interactions with dsDNA, such as phosphate recognition (Supplementary Fig. S4).

To confirm the dsDNA-binding residues observed in the $lmDegU_{DBD}$-dsDNA model, the R168, N198, and R212 residues at the putative dsDNA-binding site were individually mutated to alanine in $lmDegU_{DBD}$. Each of the three $lmDegU_{DBD}$ mutants ($lmDegU_{DBD}^{R168A}$, $lmDegU_{DBD}^{N198A}$, and $lmDegU_{DBD}^{R212A}$) exhibited lower dsDNA-binding affinity in the FP assay than $lmDegU_{DBD}$, indicating that the continuous positive patch of the $lmDegU_{DBD}$ dimer covering the R168, R212, and N198 residues mediates dsDNA recognition (Fig. 4C and Supplementary Fig. S6). Noticeably, among the three mutants, the $lmDegU_{DBD}^{R168A}$ mutant displayed the lowest dsDNA binding level, highlighting the critical role of the highly conserved, positively charged R168 residue in DNA recognition.

Contribution of the lmDegU RD to the DNA-binding capacity of lmDegU. To determine the relative contributions of the lmDegU DBD and RD to the dsDNA interaction, an FP assay was performed using the $lmDegU_{DBD}$ and $lmDegU_{RD}$ proteins containing only one domain (Figs. 1A,B and 5A). The $lmDegU_{RD}$ protein did not exhibit any detectable dsDNA binding up to a 7.8 μM concentration, whereas the $lmDegU_{DBD}$ protein obviously interacted with dsDNA (K_d, 6.7 ± 2.3 μM) (Figs. 3A and 5A). This observation indicates that the direct interaction of lmDegU with dsDNA is primarily mediated by the DBD. Interestingly, compared to $lmDegU_{DBD}$, the $lmDegU_{FL}$ protein containing the RD and DBD more potently interacted with dsDNA (K_d, 173 ± 26 nM) by ~ 39-fold in the FP assay, suggesting that the RD makes an indirect contribution to operator DNA binding. This dsDNA-binding pattern of lmDegU was recapitulated in an electrophoresis mobility shift assay (EMSA) (Fig. 5B). In the EMSA, $lmDegU_{RD}$ could not shift the dsDNA band to the $lmDegU_{RD}$-dsDNA complex band. $lmDegU_{DBD}$ interacted with dsDNA but with a partial shift to the complex band even at an 8:1 lmDegU:dsDNA molar ratio. In contrast, a complete shift was observed for $lmDegU_{FL}$, indicating that $lmDegU_{FL}$ binds dsDNA with a higher affinity than $lmDegU_{DBD}$.

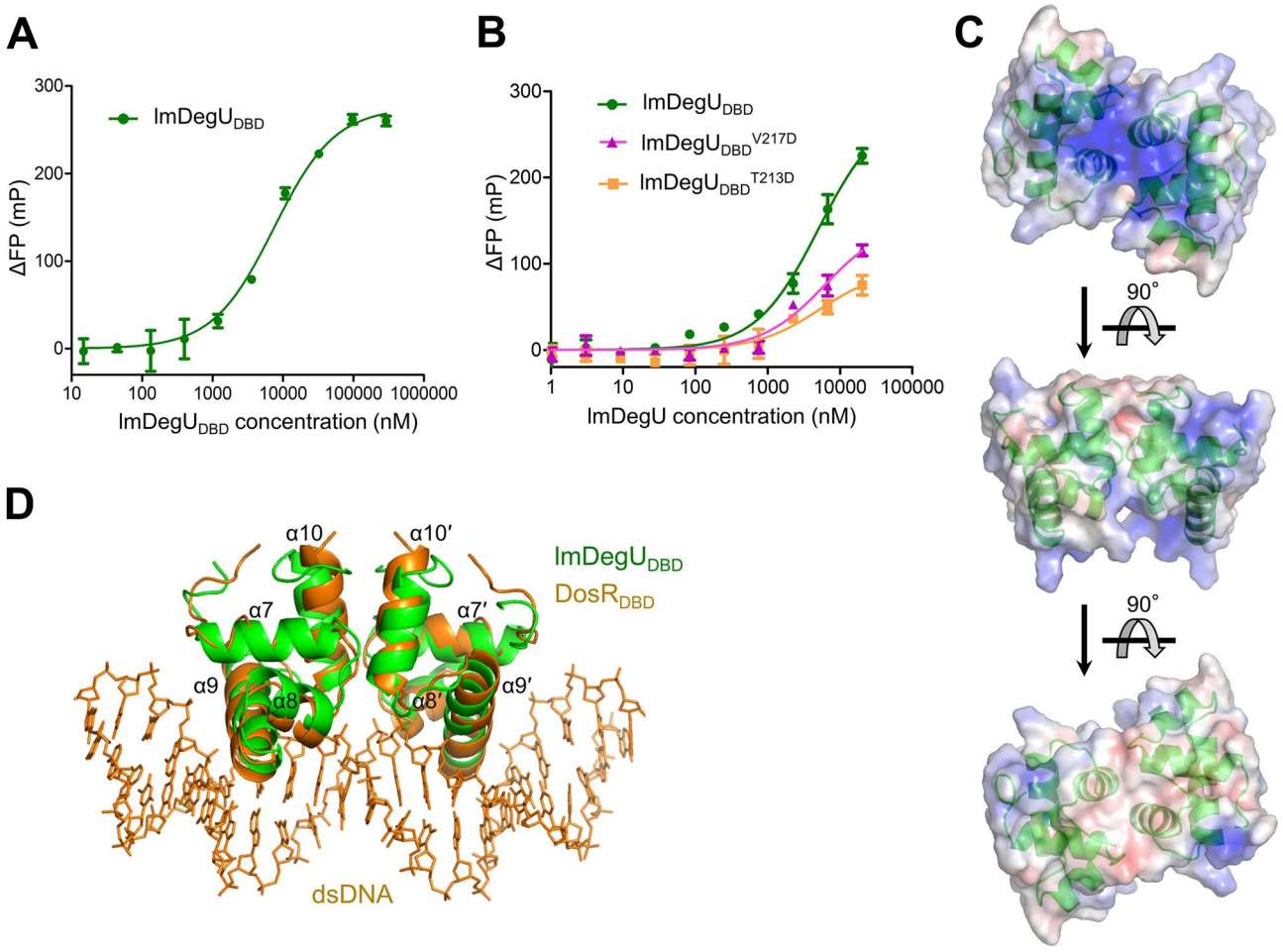

Figure 3. DNA binding by lmDegU$_{DBD}$. (**A**) Operator dsDNA-binding affinity of lmDegU$_{DBD}$ based on the FP assay. The data (means ± S.D.) are representative of four independent experiments that yielded similar results. (**B**) DNA-binding levels of lmDegU$_{DBD}$ and the dimerization-deficient mutants (lmDegU$_{DBD}^{T213D}$ and lmDegU$_{DBD}^{V217D}$) based on the FP assay. The data (means ± S.D.) are representative of three independent experiments that yielded similar results. (**C**) Surface electrostatic potentials of lmDegU$_{DBD}$. The lmDegU$_{DBD}$ dimer structure is shown as semi-transparent electrostatic potential surfaces (positive, blue; neutral, white; negative, red) with ribbons (green). The orientation of lmDegU$_{DBD}$ in the middle panel is identical to that in Fig. 2A. (**D**) Overlay of the lmDegU$_{DBD}$ dimer structure (green ribbons) on the DosR$_{DBD}$-dsDNA complex structure (DosR$_{DBD}$, orange ribbons; dsDNA, orange lines; PDB ID 1ZLK)[24]. The orientation of the lmDegU$_{DBD}$ dimer in the figure is identical to that in the middle panel in (**C**).

Phosphorylation-independent DNA-binding capacity of lmDegU. Most response regulators control their interactions with operator DNA and subsequent transcription in a phosphorylation-dependent manner[16,17]. In general, response regulators do not recognize operator DNA when they are not phosphorylated. Upon phosphorylation, response regulators enhance their operator DNA-binding capacity via a conformational change and homodimerization. In contrast to typical response regulators, the unphosphorylated lmDegU$_{FL}$ protein displayed substantial binding to the operator dsDNA with a K_d value of 173 ± 26 nM (Figs. 5A and 6). To rule out the possibility that the lmDegU$_{FL}$ protein used in the assay was already phosphorylated during expression or purification, a lmDegU$_{FL}$ mutant (lmDegU$_{FL}^{D55N}$) that cannot be phosphorylated due to a phosphorylation site mutation (D55N mutation) was generated and analyzed for dsDNA binding (Fig. 1B). The lmDegU$_{FL}^{D55N}$ mutant exhibited comparable dsDNA binding to that of lmDegU$_{FL}$ in the FP assay, confirming the ability of unphosphorylated lmDegU to recognize operator DNA (Fig. 6 and Supplementary Fig. S6).

To address any phosphorylation-mediated changes in the lmDegU-dsDNA interaction, the phosphorylated lmDegU$_{FL}$ protein was generated using acetyl phosphate as a phosphodonor, and its dsDNA binding was analyzed by an FP assay. Acetyl phosphate has been shown to phosphorylate diverse response regulators, including lmDegU, in vitro[25–27]. Unexpectedly, the phosphorylated lmDegU$_{FL}$ protein displayed essentially identical dsDNA binding to that of unphosphorylated lmDegU$_{FL}$ (Fig. 6). Moreover, mutation of the aspartate residue at the phosphorylation site (D55) to glutamate to generate the phosphomimetic lmDegU$_{FL}$ (lmDegU$_{FL}^{D55E}$) did not significantly change the dsDNA-binding affinity of lmDegU$_{FL}$ (Fig. 6 and Supplementary Fig. S6). Considering these results, we conclude that lmDegU is a unique response regulator that interacts with the operator dsDNA even in an unphosphorylated state and does not change its dsDNA-binding ability in response to phosphorylation.

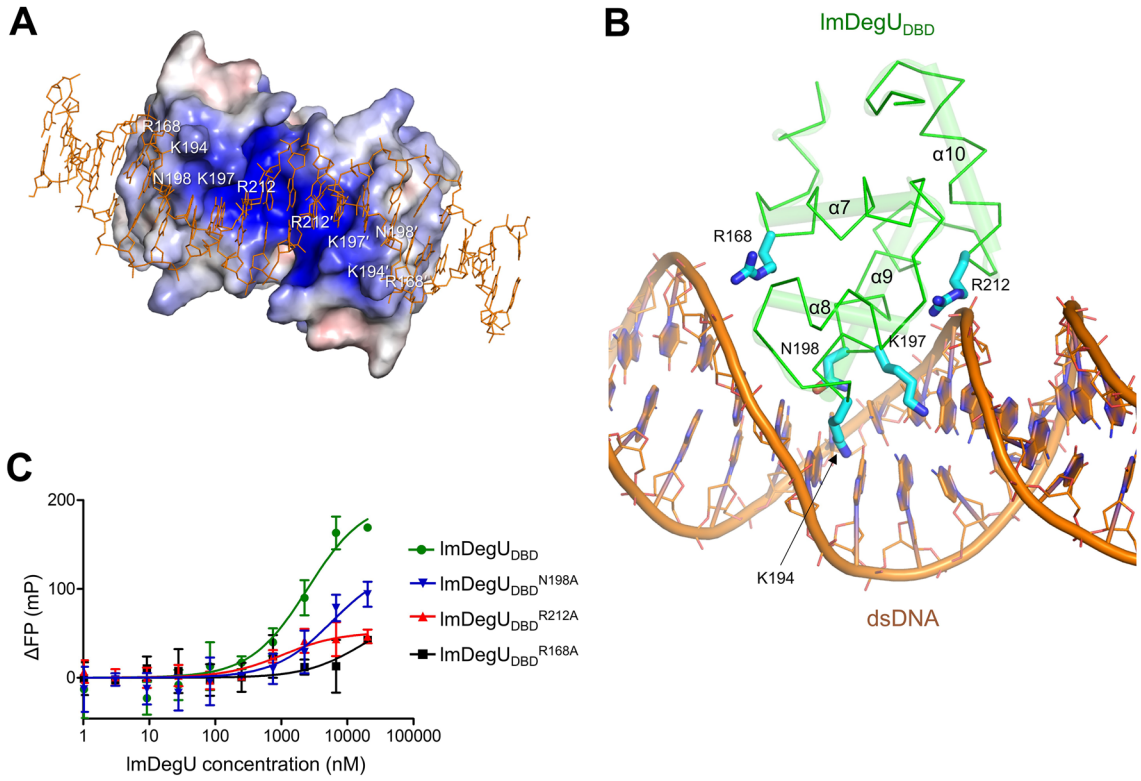

Figure 4. dsDNA-binding residues of lmDegU$_{DBD}$. (**A**) Putative dsDNA-binding residues of lmDegU$_{DBD}$ (white labels) in the model of a complex between the lmDegU$_{DBD}$ dimer (electrostatic potential surfaces) and dsDNA (orange lines). In the model, dsDNA resides on the positive electrostatic potential surface of the lmDegU$_{DBD}$ dimer. (**B**) Interactions of the lmDegU R168, K194, K197, N198, and R212 residues (cyan sticks) with dsDNA in the model of a complex between the lmDegU$_{DBD}$ monomer (green Cα traces with transparent cylindrical helices) and dsDNA (orange lines and cartoons with filled base rings). (**C**) Mutagenesis-based verification of the dsDNA-binding surface of lmDegU$_{DBD}$. The dsDNA-binding affinities of the lmDegU$_{DBD}^{R168A}$, lmDegU$_{DBD}^{N198A}$, and lmDegU$_{DBD}^{R212A}$ mutants were analyzed by the FP assay in comparison with that of lmDegU$_{DBD}$. The data (means ± S.D.) are representative of five independent experiments that yielded similar results.

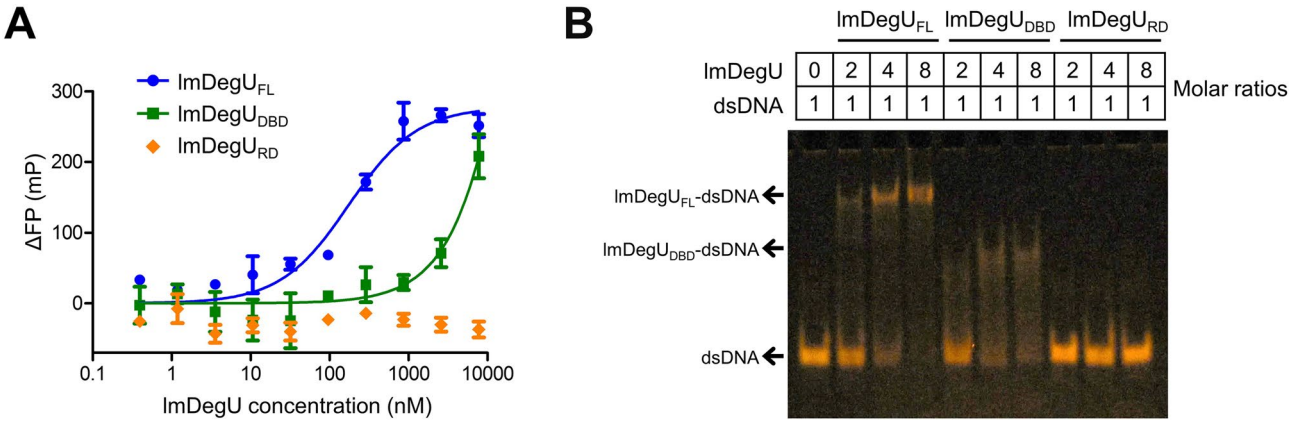

Figure 5. Enhancement of the DNA-binding capacity of lmDegU by the RD. (**A**) dsDNA-binding levels of lmDegU$_{FL}$, lmDegU$_{DBD}$, and lmDegU$_{RD}$ based on the FP assay. The data (means ± S.D.) are representative of three independent experiments that yielded similar results. (**B**) dsDNA-binding capacities of lmDegU$_{FL}$, lmDegU$_{DBD}$, and lmDegU$_{RD}$ based on the EMSA. The gel image is representative of three independent experiments that yielded similar results. The full-length gel is shown in Supplementary Fig. S11.

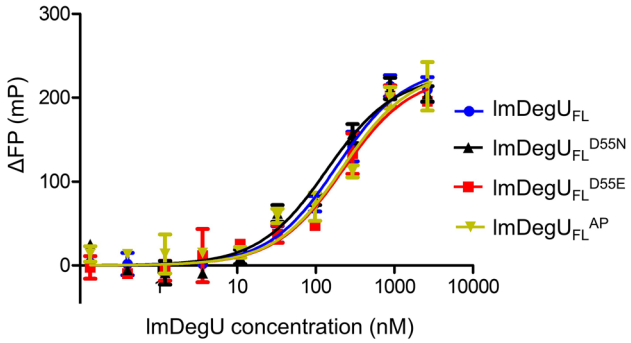

Figure 6. Similar dsDNA-binding levels of lmDegU observed irrespective of phosphorylation. The dsDNA-binding levels of lmDegU$_{FL}$, phosphorylation-incompatible lmDegU$_{FL}^{D55N}$, the lmDegU$_{FL}^{D55E}$ phosphomimetic, and acetyl phosphate-phosphorylated lmDegU$_{FL}$ (lmDegU$_{FL}^{AP}$) were determined by the FP assay. The data (means ± S.D.) are representative of five independent experiments that yielded similar results.

Despite the phosphorylation-independent lmDegU-dsDNA interaction, phosphorylation appears to modulate the lmDegU structure. In gel-filtration chromatography, the lmDegU$_{FL}^{D55E}$ phosphomimetic was eluted earlier than lmDegU$_{FL}$, suggesting that phosphorylation induces a change in the conformation or size of lmDegU (Supplementary Fig. S8). Furthermore, given that lmDegU contains the key residues (D50, T83, Y102, and K105 residues) required for phosphorylation-mediated conformational rearrangement and dimerization, it is highly likely that lmDegU undergoes the structural changes that have been reported in typical response regulators.

Discussion

lmDegU plays a key role in the transcriptional activation of GmaR protein and flagellar proteins[12]. This transcriptional regulation is mediated by the interaction of lmDegU with its operator dsDNA in the *fliN-gmaR* promoter. Our structural and biochemical studies indicate that lmDegU recognizes the operator dsDNA using the DBD in a dimeric organization. This binding is fortified by the RD. The RD-mediated increase in dsDNA-binding affinity was also reported in other NarL family members that are homologous to lmDegU. For example, full-length LiaR bound the operator dsDNA with 100-fold higher affinity than its DBD[28].

lmDegU displayed significant dsDNA-binding capacity although it was not phosphorylated. Consistently, lmDegU was demonstrated to induce flagellar and GmaR expression even without phosphorylation[12,26]. In contrast to lmDegU, VraR and NarL, which belong to the NarL family, were shown to exist in an autoinhibited conformation via RD-mediated occlusion of the DBD dimerization site or the DNA-binding site when unphosphorylated[29,30]. Thus, unphosphorylated VraR did not exhibit any detectable dsDNA binding[29]. NarL family members use phosphorylation as a key mechanism to regulate their activities. VraR changes from an inactive conformation to an active form upon phosphorylation by releasing the DBD from the RD to interact with dsDNA[29]. As a result, phosphorylation enhanced the dsDNA-binding affinity of VraR by at least 30-fold. However, lmDegU phosphorylation did not significantly improve the DNA-binding capacity, given that the lmDegU phosphomimetic and chemically phosphorylated lmDegU displayed similar DNA-binding affinities to that of the unphosphorylated lmDegU protein. This comparative analysis indicates that lmDegU displays a unique phosphorylation-independent dsDNA-binding mode that is not observed in NarL and VraR despite 30–40% sequence identities of lmDegU shared with NarL and VraR.

The interdomain helix, α6, which is located between the RD and DBD, was proposed to be a critical player that determines VraR activity[29,31]. In unphosphorylated VraR, the α6 helix tethers the RD and DBD into the inactive conformation by bridging the two domains. Upon phosphorylation-mediated activation, the α6 helix undergoes structural rearrangements to liberate the DBD for DNA binding. Interestingly, lmDegU contains an exceptionally long interdomain region (Supplementary Fig. S9). Thus, we hypothesize that the additional interdomain region positions the DBD away from the RD without an interdomain interaction in the unphosphorylated state and contributes to the adoption of the active conformation even without phosphorylation. We could not prove this hypothesis because of a technical difficulty. Specifically, a lmDegU mutant lacking the additional loop region could not be obtained due to protein instability. Future structural studies on lmDegU in both unphosphorylated and phosphorylated states are necessary to reveal the exact mechanism in which lmDegU adopts the active state without phosphorylation.

The regulation of flagellar expression by unphosphorylated lmDegU is not specific to *L. monocytogenes*. In *B. subtilis*, unphosphorylated DegU positively regulates the *fla*/*che* operon and *comK* gene for flagellar formation and genetic competence, respectively[32,33]. Another common property of unphosphorylated lmDegU and *B. subtilis* DegU (bsDegU) is that both recognize inverted repeat sequences. However, when phosphorylated, bsDegU controls the expression of another set of ~ 170 genes, including genes involved in degradative enzyme production, potentially by recognizing direct repeat sequences[34,35]. Therefore, unlike lmDegU, bsDegU is considered a molecular switch that alternatively activates transcription of two gene sets depending on phosphorylation[36]. In addition to this regulatory distinction, *L. monocytogenes* differs from *B. subtilis* in that *L. monocytogenes* lacks the *degS* gene that is required to phosphorylate DegU. Thus, *L. monocytogenes* and *B. subtilis* seem to have

undergone different evolutionary routes in the DegS-DegU system although both species belong to the same order Bacillales in the phylum Firmicutes.

lmDegU can be phosphorylated by acetyl phosphate in *L. monocytogenes*, and lmDegU phosphorylation was shown to accelerate flagellar expression[26]. However, in our binding study, phosphorylation did not enhance the dsDNA-binding affinity of lmDegU, indicating that the phosphorylation-mediated improvement in flagellar expression is not ascribed to the direct interaction of lmDegU with the operator DNA in the *fliN-gmaR* promoter. Notably, phosphorylation modulated the elution profile of lmDegU in gel-filtration chromatography, indicating that lmDegU changes its conformation or oligomeric state upon phosphorylation (Supplementary Fig. S8). These observations lead us to propose that the phosphorylation-mediated structural change in lmDegU generates a new surface that can be used to recruit an unidentified regulator and to improve motility gene expression.

Methods

Construction of the protein expression plasmid. The DNA fragment that encodes the $lmDegU_{FL}$ protein (residues 1–228) was amplified by PCR from the genomic DNA of *L. monocytogenes* ATCC 15313. The PCR product was digested using the *Nde*I and *Xma*I restriction enzymes and was inserted using T4 DNA ligase into the pET49b plasmid that was modified to express the recombinant protein in fusion with a C-terminal hexahistidine (His_6) tag. The ligation product was transformed into the *E. coli* DH5α strain. A transformant containing the $lmDegU_{FL}$ expression plasmid was verified by DNA sequencing. The $lmDegU_{RD}$ (residues 1–143) and $lmDegU_{DBD}$ (residues 159–228) expression plasmids were generated by PCR using the $lmDegU_{FL}$ expression plasmid as template DNA and by the subsequent ligation of the *Bam*HI- and *Sal*I-digested PCR product into the pET49b vector, which was modified to express recombinant protein with an N-terminal His_6 tag and a subsequent thrombin or TEV protease cleavage site[37]. The lmDegU gene in the expression plasmid was mutated using the site-directed mutagenesis protocol (Agilent).

Protein expression and purification. For protein overexpression, the lmDegU expression plasmid was transformed into the *E. coli* BL21 (DE3) strain. *E. coli* BL21 (DE3) cells containing the lmDegU expression plasmid were grown at 37 °C in LB broth containing 100 μM kanamycin. When the optical density of the culture at 600 nm reached 0.6, the culture was supplemented with 1 mM isopropyl β-D-1-thiogalactopyranoside for overexpression. The cells were further grown at 18 °C for 18 h. The resulting cells were lysed by sonication in a solution containing 50 mM Tris, pH 8.0, 300 mM sodium chloride, and 5 mM β-mercaptoethanol. The lmDegU protein was first purified from the cell lysate by Ni–NTA affinity chromatography through imidazole-mediated elution. The eluted $lmDegU_{FL}$, $lmDegU_{RD}$, and $lmDegU_{DBD}$ proteins were dialyzed against solutions of different compositions (50 mM Tris, pH 8.0, 300 mM sodium chloride, and 5 mM β-mercaptoethanol for $lmDegU_{FL}$; 20 mM Tris, pH 8.0, and 5 mM β-mercaptoethanol for $lmDegU_{RD}$; 20 mM Hepes, pH 7.4, 300 mM sodium chloride, and 5 mM β-mercaptoethanol for $lmDegU_{DBD}$). The dialyzed $lmDegU_{RD}$ and $lmDegU_{DBD}$ proteins were subjected to digestion by TEV protease and thrombin, respectively, to cleave the His_6 tag. The tag-free $lmDegU_{RD}$ and $lmDegU_{DBD}$ proteins were further purified by gel-filtration chromatography using a Superdex 200 16/600 column (GE Healthcare) in solutions with different compositions (20 mM Tris, pH 8.0, and 150 mM sodium chloride for $lmDegU_{RD}$; 20 mM Hepes, pH 7.4, 300 mM sodium chloride, and 5 mM β-mercaptoethanol for $lmDegU_{DBD}$).

Crystallization and X-ray diffraction. The purified $lmDegU_{DBD}$ protein was concentrated to 11.6 mg/ml for crystallization. $lmDegU_{DBD}$ crystals were obtained by performing a sitting-drop vapor-diffusion method using a 24-well Cryschem plate (Hampton Research). For crystallization, 0.5 μl of the $lmDegU_{DBD}$ protein was mixed with 0.5 μl of a well solution containing 22% PEG 3350 and 0.1 M Tris, pH 8.0, and was equilibrated via vapor diffusion against 500 μl of the well solution at 18 °C. A $lmDegU_{DBD}$ crystal was briefly soaked in 25% glycerol, 24% PEG 3350, and 0.1 M Tris, pH 8.0, for cryoprotection and flash-cooled at − 173 °C under a nitrogen gas stream. X-ray diffraction data from a single $lmDegU_{DBD}$ crystal were collected at beamline 7A, Pohang Accelerator Laboratory. The X-ray diffraction data were processed and scaled using the HKL2000 program[38]. The data collection statistics are listed in Supplementary Table S1.

Structure determination and analysis. The $lmDegU_{DBD}$ structure was determined by molecular replacement with the Phaser program[39]. Molecular replacement was performed using the crystal structure of the DNA-binding domain of *Enterococcus faecalis* LiaR (PDB ID 4WSZ) as a search model[40]. The initial model of $lmDegU_{DBD}$ was iteratively modified and refined using the Coot and phenix.refine programs, respectively[41,42]. TLS refinement was performed using 6 TLS groups during the refinement runs to generate the $lmDegU_{DBD}$ structure. The final structure of $lmDegU_{DBD}$ exhibited good geometry and stereochemistry without Ramachandran plot outliers. The $lmDegU_{DBD}$ structure has relatively high B-factors (average B-factor, 76.6 Å), presumably due to inherent intersubunit flexibility that is caused by the low dimerization affinity. The refinement statistics are listed in Supplementary Table S1.

Chemical crosslinking of $lmDegU_{DBD}$. $lmDegU_{DBD}$ dimerization was verified by crosslinking. For chemical crosslinking, 5 μg of $lmDegU_{DBD}$ or its mutants in 5 μl of 20 mM Hepes, pH 7.4, 300 mM sodium chloride, and 5 mM β-mercaptoethanol was incubated with a 5-μl mixture of 80 mM 1-ethyl-3-(3-dimethylaminopropyl) carbodiimide hydrochloride (EDC) and 80 mM N-hydroxysulfosuccinimide (Sulfo-NHS) for 5 min at room temperature. The crosslinking reaction was stopped using 5 μl of a solution containing 500 mM Tris, pH 8.0, and 20 mM β-mercaptoethanol. The crosslinked protein was analyzed by SDS-PAGE and stained using Coomassie Brilliant Blue G-250 dye.

FP assay. To determine the dsDNA-binding affinity of lmDegU, an FP assay was performed. For the FP assay, an operator dsDNA was generated by annealing a fluorescein-labeled 36-mer ssDNA fragment (5′-CGA GTAGGTCAAAAGGATTGGGTATGAAGAACCTTT-3′ in the *fliN-gmaR* promoter site) and its unlabeled complementary ssDNA counterpart (5′-AAAGGTTCTTCATACCCAATCCTTTTGACCTACTCG-3′)[12]. The resultant 36-bp operator dsDNA (0.3 nM) was incubated with lmDegU protein at various concentrations for 30 min at 18 °C in 20 mM Tris, pH 7.0, 50 mM sodium chloride, and 5 mM β-mercaptoethanol[12]. The fluorescence polarization of the fluorescein-labeled dsDNA in the absence and presence of lmDegU protein was measured using an Infinite F200 PRO instrument (Tecan) and analyzed with the Prism 5 software (GraphPad) using a one-site binding model to derive a K_d value for the lmDegU-dsDNA interaction.

EMSA. To qualitatively analyze the lmDegU-dsDNA interaction, an EMSA was performed using the lmDegU protein and unlabeled 36-bp operator dsDNA. The lmDegU protein was incubated with the operator dsDNA at various molar ratios at 18 °C for 30 min. The protein-dsDNA mixture was electrophoresed in a polyacrylamide gel using Tris–borate-EDTA running buffer. DNA bands in the electrophoretic gel were visualized by ethidium bromide.

Gel-filtration chromatography analysis. Gel-filtration chromatography was performed to analyze the molecular size and folding of lmDegU. The lmDegU protein in 50 mM Tris, pH 8.0 (or 20 mM Hepes, pH 7.4), 300 mM sodium chloride, and 5 mM β-mercaptoethanol was loaded onto a Superdex 200 10/300 column. Protein elution was monitored by measuring the UV absorbance at 280 nm. For comparison, a gel-filtration standard solution (Bio-Rad) was independently loaded onto the column.

Circular dichroisms (CD) spectroscopy. To verify that mutation does not affect protein folding, CD spectra were obtained using $lmDegU_{FL}$, $lmDegU_{DBD}$, and their mutants (0.5 mg/ml). The purified lmDegU protein was dialyzed against a solution containing 50 mM Tris, pH 8.0, 300 mM sodium fluoride, and 5 mM β-mercaptoethanol and then subjected to CD measurement. CD spectra from 190 to 260 nm were recorded at 25 °C using a J-1500 CD spectropolarimeter (Jasco) at the Korea Basic Science Institute (Ochang, Korea), with a step resolution of 0.1 nm, a bandwidth of 1 nm, and a response time of 1 s.

Structure deposition. The atomic coordinates and the structure factors for $lmDegU_{DBD}$ (PDB ID 7X1K) have been deposited in the Protein Data Bank (http://www.rcsb.org).

Received: 13 November 2021; Accepted: 7 June 2022
Published online: 07 July 2022

References

1. Freitag, N. E., Port, G. C. & Miner, M. D. *Listeria monocytogenes*—From saprophyte to intracellular pathogen. *Nat. Rev. Microbiol.* **7**, 623–628 (2009).
2. Chaturongakul, S., Raengpradub, S., Wiedmann, M. & Boor, K. J. Modulation of stress and virulence in *Listeria monocytogenes*. *Trends Microbiol.* **16**, 388–396 (2008).
3. van der Veen, S., Moezelaar, R., Abee, T. & Wells-Bennik, M. H. The growth limits of a large number of *Listeria monocytogenes* strains at combinations of stresses show serotype–and niche-specific traits. *J. Appl. Microbiol.* **105**, 1246–1258 (2008).
4. Cartwright, E. J. *et al.* Listeriosis outbreaks and associated food vehicles, United States, 1998–2008. *Emerg. Infect. Dis.* **19**, 1–9 (2013) (**quiz 184**).
5. Zhu, Q., Gooneratne, R. & Hussain, M. A. *Listeria monocytogenes* in fresh produce: Outbreaks, prevalence and contamination levels. *Foods* **6**, 21 (2017).
6. Ramaswamy, V. *et al.* Listeria—review of epidemiology and pathogenesis. *J. Microbiol. Immunol. Infect.* **40**, 4–13 (2007).
7. Peel, M., Donachie, W. & Shaw, A. Temperature-dependent expression of flagella of *Listeria monocytogenes* studied by electron microscopy, SDS-PAGE and western blotting. *J. Gen. Microbiol.* **134**, 2171–2178 (1988).
8. Tilney, L. G. & Portnoy, D. A. Actin filaments and the growth, movement, and spread of the intracellular bacterial parasite, *Listeria monocytogenes*. *J. Cell Biol.* **109**, 1597–1608 (1989).
9. Williams, T., Joseph, B., Beier, D., Goebel, W. & Kuhn, M. Response regulator DegU of *Listeria monocytogenes* regulates the expression of flagella-specific genes. *FEMS Microbiol. Lett.* **252**, 287–298 (2005).
10. Kamp, H. D. & Higgins, D. E. A protein thermometer controls temperature-dependent transcription of flagellar motility genes in *Listeria monocytogenes*. *PLoS Pathog.* **7**, e1002153 (2011).
11. Shen, A., Higgins, D. E. & Panne, D. Recognition of AT-rich DNA binding sites by the MogR repressor. *Structure* **17**, 769–777 (2009).
12. Kamp, H. D. & Higgins, D. E. Transcriptional and post-transcriptional regulation of the GmaR antirepressor governs temperature-dependent control of flagellar motility in *Listeria monocytogenes*. *Mol. Microbiol.* **74**, 421–435 (2009).
13. Shen, A., Kamp, H. D., Grundling, A. & Higgins, D. E. A bifunctional O-GlcNAc transferase governs flagellar motility through anti-repression. *Genes Dev.* **20**, 3283–3295 (2006).
14. Gueriri, I. *et al.* The DegU orphan response regulator of *Listeria monocytogenes* autorepresses its own synthesis and is required for bacterial motility, virulence and biofilm formation. *Microbiology* **154**, 2251–2264 (2008).
15. Grundling, A., Burrack, L. S., Bouwer, H. G. & Higgins, D. E. *Listeria monocytogenes* regulates flagellar motility gene expression through MogR, a transcriptional repressor required for virulence. *Proc. Natl. Acad. Sci. USA.* **101**, 12318–12323 (2004).
16. Krell, T. *et al.* Bacterial sensor kinases: Diversity in the recognition of environmental signals. *Annu. Rev. Microbiol.* **64**, 539–559 (2010).
17. Padilla-Vaca, F., Mondragon-Jaimes, V. & Franco, B. General aspects of two-component regulatory circuits in bacteria: Domains, signals and roles. *Curr. Protein Pept. Sci.* **18**, 990–1004 (2017).

18. Murray, E. J., Kiley, T. B. & Stanley-Wall, N. R. A pivotal role for the response regulator DegU in controlling multicellular behaviour. *Microbiology* **155**, 1–8 (2009).
19. Msadek, T. *et al.* Signal transduction pathway controlling synthesis of a class of degradative enzymes in *Bacillus subtilis*: Expression of the regulatory genes and analysis of mutations in degS and degU. *J. Bacteriol.* **172**, 824–834 (1990).
20. Glaser, P. *et al.* Comparative genomics of Listeria species. *Science* **294**, 849–852 (2001).
21. Mauder, N., Williams, T., Fritsch, F., Kuhn, M. & Beier, D. Response regulator DegU of *Listeria monocytogenes* controls temperature-responsive flagellar gene expression in its unphosphorylated state. *J. Bacteriol.* **190**, 4777–4781 (2008).
22. Mistry, J. *et al.* Pfam: The protein families database in 2021. *Nucleic Acids Res.* **49**, D412–D419 (2021).
23. Lin, A. V. & Stewart, V. Functional roles for the GerE-family carboxyl-terminal domains of nitrate response regulators NarL and NarP of *Escherichia coli* K-12. *Microbiology* **156**, 2933–2943 (2010).
24. Wisedchaisri, G. *et al.* Structures of *Mycobacterium tuberculosis* DosR and DosR-DNA complex involved in gene activation during adaptation to hypoxic latency. *J. Mol. Biol.* **354**, 630–641 (2005).
25. McCleary, W. R. & Stock, J. B. Acetyl phosphate and the activation of two-component response regulators. *J. Biol. Chem.* **269**, 31567–31572 (1994).
26. Gueriri, I., Bay, S., Dubrac, S., Cyncynatus, C. & Msadek, T. The Pta-AckA pathway controlling acetyl phosphate levels and the phosphorylation state of the DegU orphan response regulator both play a role in regulating *Listeria monocytogenes* motility and chemotaxis. *Mol. Microbiol.* **70**, 1342–1357 (2008).
27. Cairns, L. S., Martyn, J. E., Bromley, K. & Stanley-Wall, N. R. An alternate route to phosphorylating DegU of *Bacillus subtilis* using acetyl phosphate. *BMC Microbiol.* **15**, 78 (2015).
28. Jani, S. *et al.* Low phosphatase activity of LiaS and strong LiaR-DNA affinity explain the unusual LiaS to LiaR in vivo stoichiometry. *BMC Microbiol.* **20**, 104 (2020).
29. Leonard, P. G., Golemi-Kotra, D. & Stock, A. M. Phosphorylation-dependent conformational changes and domain rearrangements in *Staphylococcus aureus* VraR activation. *Proc. Natl. Acad. Sci. USA.* **110**, 8525–8530 (2013).
30. Eldridge, A. M., Kang, H. S., Johnson, E., Gunsalus, R. & Dahlquist, F. W. Effect of phosphorylation on the interdomain interaction of the response regulator, NarL. *Biochemistry* **41**, 15173–15180 (2002).
31. Davlieva, M. *et al.* An adaptive mutation in *Enterococcus faecium* liar associated with antimicrobial peptide resistance mimics phosphorylation and stabilizes LiaR in an activated state. *J. Mol. Biol.* **428**, 4503–4519 (2016).
32. Tsukahara, K. & Ogura, M. Promoter selectivity of the *Bacillus subtilis* response regulator DegU, a positive regulator of the fla/che operon and sacB. *BMC Microbiol.* **8**, 8 (2008).
33. Hamoen, L. W., Van Werkhoven, A. F., Venema, G. & Dubnau, D. The pleiotropic response regulator DegU functions as a priming protein in competence development in *Bacillus subtilis*. *Proc. Natl. Acad. Sci. USA.* **97**, 9246–9251 (2000).
34. Mader, U. *et al. Bacillus subtilis* functional genomics: Genome-wide analysis of the DegS-DegU regulon by transcriptomics and proteomics. *Mol. Genet. Genomics* **268**, 455–467 (2002).
35. Ogura, M., Yamaguchi, H., Yoshida, K., Fujita, Y. & Tanaka, T. DNA microarray analysis of *Bacillus subtilis* DegU, ComA and PhoP regulons: An approach to comprehensive analysis of *B. subtilis* two-component regulatory systems. *Nucleic Acids Res.* **29**, 3804–3813 (2001).
36. Dahl, M. K., Msadek, T., Kunst, F. & Rapoport, G. The phosphorylation state of the DegU response regulator acts as a molecular switch allowing either degradative enzyme synthesis or expression of genetic competence in *Bacillus subtilis*. *J. Biol. Chem.* **267**, 14509–14514 (1992).
37. Park, S. C. *et al.* Activation of the *Legionella pneumophila* LegK7 effector kinase by the host MOB1 protein. *J. Mol. Biol.* **433**, 166746 (2021).
38. Otwinowski, Z. & Minor, W. Processing x-ray diffraction data collected in oscillation mode. *Methods Enzymol.* **276**, 307–326 (1997).
39. McCoy, A. J. *et al.* Phaser crystallographic software. *J. Appl. Crystallogr.* **40**, 658–674 (2007).
40. Davlieva, M. *et al.* A variable DNA recognition site organization establishes the LiaR-mediated cell envelope stress response of enterococci to daptomycin. *Nucleic Acids Res.* **43**, 4758–4773 (2015).
41. Adams, P. D. *et al.* PHENIX: A comprehensive Python-based system for macromolecular structure solution. *Acta Crystallogr. Sect. D Biol. Crystallogr.* **66**, 213–221 (2010).
42. Emsley, P. & Cowtan, K. Coot: Model-building tools for molecular graphics. *Acta Crystallogr. Sect. D Biol. Crystallogr.* **60**, 2126–2132 (2004).

Acknowledgements

We thank beamline scientists at beamline 7A of the Pohang Accelerator Laboratory for their help with X-ray diffraction. This study was supported by the research grant (2019R1A2C1002100 to SIY) of the National Research Foundation of Korea (NRF) through the Ministry of Science and ICT.

Author contributions

S.I.Y. conceived and coordinated the research. H.B.O. and S.I.Y. designed the experiments. H.B.O., S.J.L., and S.I.Y. performed the experiments and analyzed the data. H.B.O. and S.I.Y. wrote the manuscript.

Competing interests

The authors declare no competing interests.

Additional information

Supplementary Information The online version contains supplementary material available at https://doi.org/10.1038/s41598-022-14459-5.

Correspondence and requests for materials should be addressed to S.I.Y.

Reprints and permissions information is available at www.nature.com/reprints.

Publisher's note Springer Nature remains neutral with regard to jurisdictional claims in published maps and institutional affiliations.